A Porphyrin–Fullerene Dyad with a Supramolecular "Double-Cable" Structure as a Novel Electron Acceptor for Bulk Heterojunction Polymer Solar Cells

Chien-Lung Wang, Wen-Bin Zhang, Ryan M. Van Horn, Yingfeng Tu, Xiong Gong, Stephen Z. D. Cheng,* Yanming Sun, Minghong Tong, Junghwa Seo, Ben B. Y. Hsu, and Alan J. Heeger*

Bulk heterojunction (BHJ) polymer solar cells (PSCs) offer a promising, low-cost, large-area, flexible, light-weight, clean, and quiet alternative energy source for both indoor and outdoor applications.[1–4] Power conversion efficiencies (PCEs) in response to solar AM1.5 radiation as high as 6–8% have been reported for BHJ PSCs.[5,6] In order to achieve PCEs over 10%, BHJ materials capable of generating higher short circuit current (J_{sc}) and larger open circuit voltage (V_{oc}) are required.[7,8] One approach to increase J_{sc} and V_{oc} is to develop low-bandgap semiconducting polymers with deeper HOMO (highest occupied molecular orbital) energies.[9–12] An alternative approach is to develop new electron acceptors with higher LUMO (lowest unoccupied molecular orbital) energies.[13–15] The pathway to low-bandgap semiconducting polymers with deeper HOMOs is now well established, and BHJ PSCs fabricated using these novel semiconducting polymers have demonstrated high PCEs.[5–12] On the other hand, the development of novel electron acceptors is behind the pace of the progress of development of PSCs. The synthesis of novel electronic acceptors with controlled molecular electronic structures and solid-state supramolecular structures is urgently required, among which a supramolecular "double-cable" structure consisiting of two separated channels for charge transport is particularly desirable in generating high J_{sc} and thus, higher PCEs.[13–16]

The construction of supramolecular structures of the π-conjugated molecules via self-assembly has been recognized as an important approach to manipulate their optical and electronic properties to generate "supramolecular electronics".[17–20] Specific device configuration often requires explicit supramolecular arrangements of these electronically active molecular segments. For example, to achieve high PCEs in PSCs, a bicontinous network with large donor/acceptor (D/A) interface and separate electron- and hole-transporting channels is highly desired.[2] The double-cable structure has thus been proposed, typically composed of a p-type conjugated polymer donor backbone tethered by n-type acceptor moieties, such as [60]fullerene (C_{60}).[16,21–26] It was anticipated that this type of materials could self-assemble into phase-separated D/A nanostructures with ambipolar transporting properties. However, the traditional grafting approach lacks precise control over both primary chemical and secondary physical structures, which compromises the device performance. So far, there is no well-defined, physical double-cable structure in polymers reported with improved PCEs.

In this communication, we report the design and synthesis of a porphyrin–fullerene dyad (PFD1, **Scheme 1**) and unambiguously demonstrate that it self-assembles into a well-defined 3D structure with alternating arrangements of separate domains of porphyrin and C_{60} in the solid state, which can be deemed as a prototype supramolecular double-cable structure in solid state. The π–π stacking of porphyrin moieties form columns of the planar donor. In the absence of a bulky neighboring group, the C_{60} moieties are able to interact in between the columns to form continuous domains of C_{60}. The photoelectronic property and preliminary results on the device performances of BHJ PSCs fabricated using these dyads as electron acceptors are also reported. Ultrafast charge transfer and charge generation were observed from the blending of semiconducting polymers with PFD1, which indicates that PFD1 is an excellent electron acceptor for PSCs. More importantly, the high J_{sc} were observed from BHJ PSCs, suggesting that a controlled ambipolar transporting property within the electron acceptor domain can lead to improved photovoltaic performances.

The molecular structures of PFD1 as well as poly[(4,4'-bis(2-ethylhexyl)dithieno[3,2-b:2',3'-d]silole)-2,6-diyl-alt-(4,7-bis(2-thienyl)-2,1,3-benzothiadiazole)-5,5'-diyl] (SiPCPDTBT)[27] and [6,6]-phenyl-C_{61}-butyric acid methyl ester (PCBM) are shown in Scheme 1. PFD1 has been well characterized by ^{1}H NMR, ^{13}C NMR, UV-vis spectroscopy, and matrix-assisted laser desorption/ionization–time of flight (MALDI-TOF) mass spectrometry to establish its chemical identity and purity. The detailed synthetic procedure and molecular characterization data are described in the Supporting Information. PFD1 was synthesized by reacting 5,10,15,20-tetra-(*p*-hydroxyphenyl) porphyrin first with 3,4,5-tris(dodecyloxy) benzoic acid and then with a carboxylic acid derivative of C_{60} (**2**) using Steglich esterification (Scheme S1, Supporting Information). Comparing the ^{1}H NMR spectrum of PFD1 with that of the porphyrin precursor (**1**),

C.-L. Wang, Dr. W.-B. Zhang, Dr. R. M. Van Horn, Dr. Y. Tu, Prof. X. Gong, Prof. S. Z. D. Cheng
College of Polymer Science and Polymer Engineering
The University of Akron
Akron, OH 44325, USA
E-mail: xgong@uakron.edu; scheng@uakron.edu
Dr. Y. Sun, Dr. M. Tong, Dr. J. Seo, B. B. Y. Hsu, Prof. A. J. Heeger
Center for Polymers and Organic Solids
University of California Santa Barbara
Santa Barbara, CA 93106, USA

DOI: 10.1002/adma.201100399

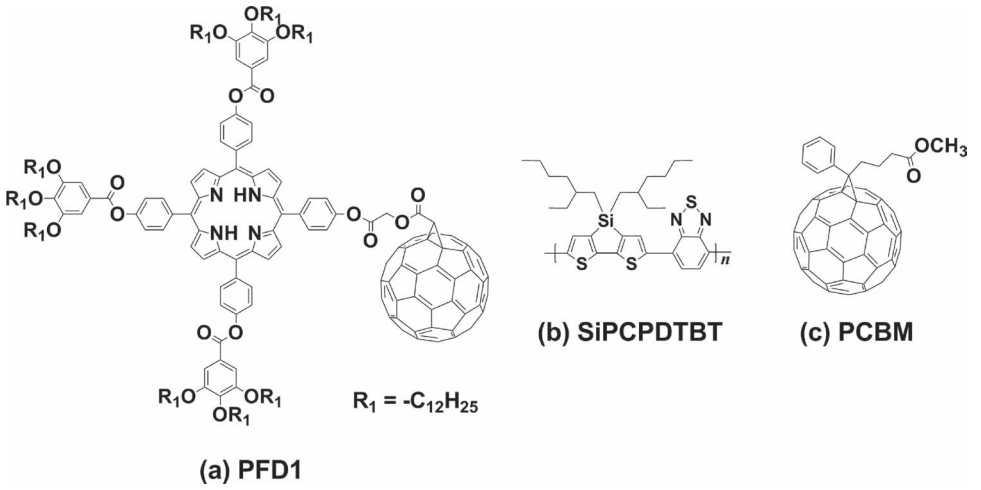

Scheme 1. a) Molecular structures of PFD1, b) SiPCPDTBT, and c) PCBM.

the two doublet peaks at δ = 8.09 and 7.21 ppm (Figure S2a, Supporting Information), which are due to the protons on the *p*-hydroxyphenyl group of **1**, shifted downfield to δ = 8.29 ppm and 7.65 ppm (Figure S1a, Supporting Information). This indicates the formation of an ester bond between the porphyrin and C_{60} moieties. In addition, the singlet peaks at δ = 5.41 ppm (2H) and δ = 4.88 ppm (1H) in Figure S1a (Supporting Information) are characteristic of the protons at the methylene and methine groups on the C_{60} arm of PFD1, and multiple peaks between δ = 135 and 145 ppm in the ^{13}C-NMR spectrum of PFD1 (Figure S1b, Supporting Information), are characteristic of the sp^2 carbons on the C_{60} moiety. Since these characteristic peaks are not observed in the ^{1}H NMR and ^{13}C NMR spectra of **1** (Figures S2a,b, Supporting Information), the presence of the C_{60} moiety on PFD1 can be confirmed. The well-defined structures were further proven by the MALDI-TOF mass spectra (Figures S1c,S2c, Supporting Information). The observed mass-to-charge (*m*/*z*) values of 3466.78 and 2648.02 closely match the calculated $[M + H]^+$ value of PFD1 (3466.95 Da) and the $[M]^+$ value of **1** (2647.95 Da), respectively. Considering that MALDI-TOF mass spectroscopy can detect impurities as low as 1%, the single distribution observed in the mass spectrum of PFD1 also proved the purity of PFD1. These results clearly indicate the success of the reaction and confirm the chemical identity and purity of PFD1.

The phase behavior of PFD1 was studied utilizing differential scanning calorimetric (DSC) experiments. A single first-order transition during heating can be observed with an onset temperature of 160 °C at a heating rate of 5 °C min^{-1} (Figure S3a, Supporting Information). The formation of the ordered phase is not observed during the subsequent cooling process at the same rate, indicating that the transformation to the ordered phase is kinetically slow. Nevertheless, it is still achievable through annealing. In thermogravimetric measurements, the 1% weight loss temperature was observed at 338 °C at a heating rate of 10 °C min^{-1} (Figure S3b, Supporting Information), suggesting the high thermal stability of the compound.

To determine the structure of the ordered phase, 2D wide angle X-ray diffraction (WAXD) and electron diffraction (ED) experiments were performed. **Figure 1**a is a 2D WAXD pattern of mechanically oriented PFD1 dyads with the X-ray beam direction perpendicular to the mechanically sheared direction. The layer diffractions can be seen along the equator direction, which can be assigned as the (100) and its higher order diffractions. Along the meridian direction, the (020) and (040) diffractions can be observed. Figure 1b shows an ED pattern with the (0kl) diffractions in the b^*c^* plane. Along the equator direction, the (020) and (040) diffractions can be observed, corresponding to the diffractions along the meridian direction in the 2D WAXD pattern of Figure 1a, while in the meridian direction of the ED pattern, the (004) diffraction appears. Thus, it is the ED pattern with the [100] zone. Based on these experimental results, we can deduce an orthorhombic unit cell with a = 3.96 nm, b = 3.60 nm, c = 1.40 nm, and $\alpha = \beta = \gamma = 90°$. The molecular packing of this ordered structure was elucidated by computer simulation via the Accelrys Cerius^2 package using the universal force field to achieve the minimum packing free energy. The results are shown in Figure 1c (top view) and d (side view), where the columns of porphyrin moieties along the *c*-axis and the C_{60} channels along the same direction can be clearly seen. This well-defined alternating arrangement of continuous donor and acceptor domains is unprecedented and promising as potential supramolecular double-cable materials.

The normalized UV-vis absorption spectra of thin films of pristine PFD1, PCBM, SiPCPDTBT, and the blend of SiPCPDTBT:PFD1 (1.0:0.7) are shown in **Figure 2**a for comparison. The absorption band peaked at 420 nm for PFD1 results from the HOMO–LUMO transition of the porphyrin moiety. In addition, the absorption band with peaks in the region from 500 nm to 700 nm is known to arise from the lowest energy interband transition (across the bandgap) of porphyrin.[28] The absorption centered in the range of 300–600 nm for PFD1 is more intense than that of PCBM in the same range of wavelengths, indicating that PFD1 possesses a higher light-harvesting efficiency than PCBM in PSCs. The absorption spectrum of the SiPCPDTBT:PFD1 BHJ material is essentially a superposition of the absorption spectra of SiPCPDTBT and PFD1. Adding 40% w/w of PFD1 does not significantly alter

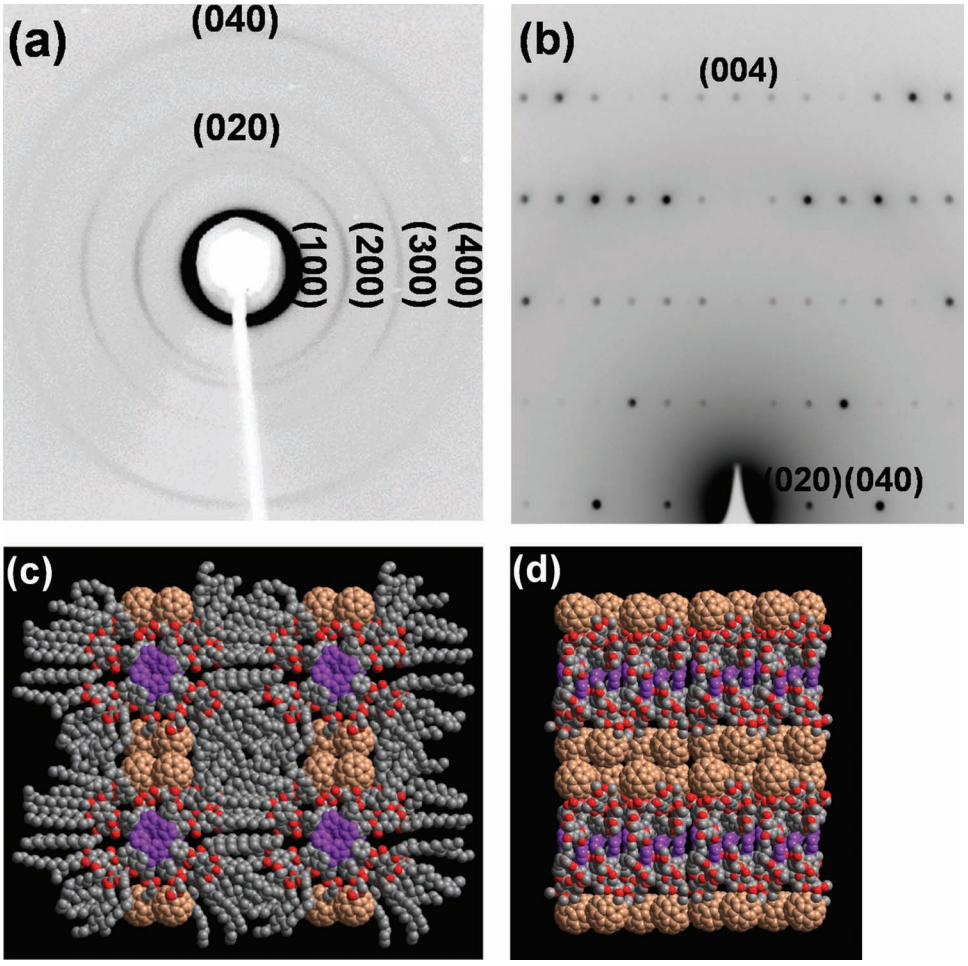

Figure 1. a) 2D WAXD pattern of the orthorhombic crystalline phase of PFD1. b) ED pattern of the orthorhombic crystalline phase of PFD1. c) Top view and d) side view of an energy-minimized model of the orthorhombic crystalline phase of PFD1. The models are built based on molecular mechanics simulation and the experimental diffraction data (purple, porphyrin core; brown, C_{60}).

the absorption of SiPCPDTBT. Meanwhile, the absorption from 360 nm to 480 nm appeared in the spectrum of SiPCPDTBT:PFD1 originates from PFD1.

Figure 2b shows the high binding energy cutoff (E_{cutoff}), while the inset of Figure 2b illustrates the HOMO region (0–5 eV) obtained from the UV photoelectron spectroscopy (UPS) spectra of the PFD1 thin film. The abscissa is the binding energy relative to the Fermi energy (E_F) of Au, which is defined by the energy of the electron before excitation relative to the vacuum level. The HOMO energy is determined to be 6.54 ± 0.03 eV based on the following formula $E_{HOMO} = h\nu - (E_{cutoff} - E_{onset})$ with the incident photon energy of $h\nu = 21.2$ eV, the E_{cutoff}, and the E_{onset} (the onset of the PFD1 film relative to the E_F of Au).[29,30] The LUMO energies were calculated using the HOMO level and the optical gap (E_g) obtained in the UV-vis absorption spectra (Figure 2a). For PFD1, E_{LUMO} is thus 3.96 ± 0.03 eV. According to the concept of band alignment between electron donors and electron acceptors in PSCs,[1–4] one might expect that photo-induced electron transfer between SiPCPDTBT and PFD1 would be efficient because of the large difference between the LUMO energies of SiPCPDTBT and PFD1.[2–4]

Furthermore, time-resolved photoinduced absorption (PIA) of the SiPCPDTBT:PFD1 (1.0:0.7) thin film was studied and compared with that of pristine SiPCPDTBT. **Figure 3**a shows the comparison of the dynamics of time-resolved PIA between pristine SiPCPDTBT and the SiPCPDTBT:PFD1 thin films. The spectra were obtained by probing at 4.6 μm and pumping at 800 nm, where SiPCPDTBT has strong absorption[27,31] but PFD1 has negligible absorption (Figure 2a). Relatively fast decay is observed in SiPCPDTBT in this mid-IR spectral region where the polaron signatures of SiPCPDTBT are detected.[31–33] The much longer polaron lifetime in SiPCPDTBT:PFD1 compared with that in pristine SiPCPDTBT indicates the photogeneration of long-lived carriers, which is consistent with efficient electron transfer from SiPCPDTBT to PFD1.[31–33] These data are in good agreement with the results obtained from typical polymer/fullerene BHJ materials where electron transfer from semiconducting polymer donor to fullerene acceptor increases the lifetime of photogenerated mobile charge carriers.[2]

The specific difference between PFD1 and PCBM was studied using time-resolved PIA in pristine PFD1 and PCBM with photoexcitation at 400 nm, where both PFD1 and PCBM

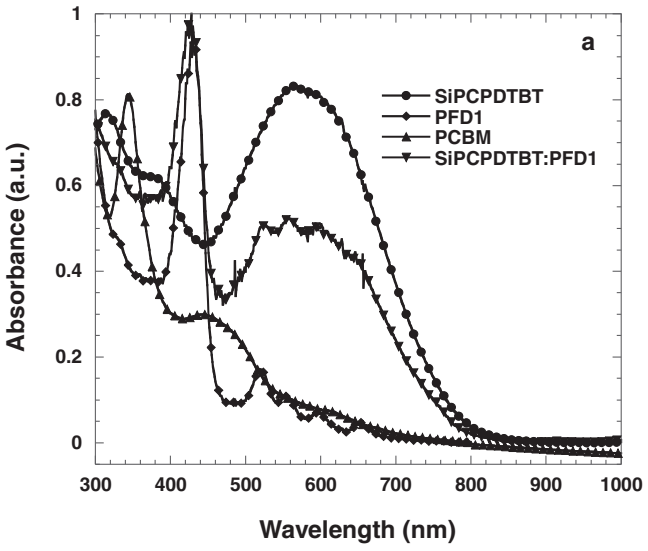

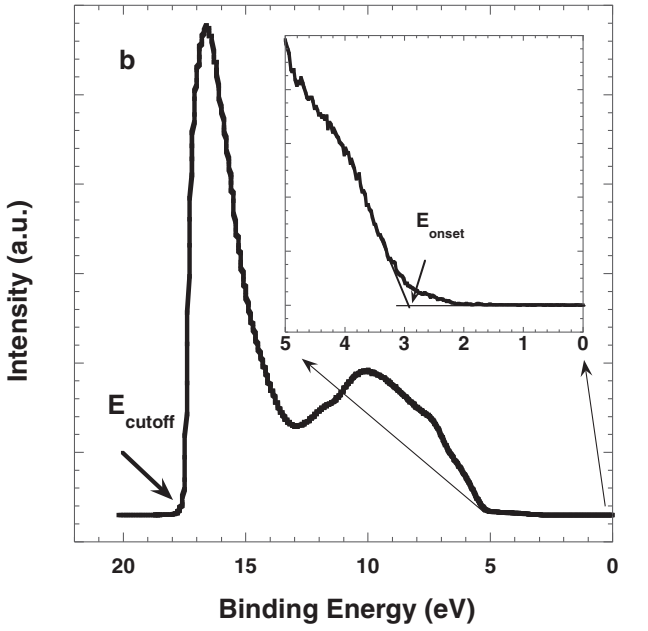

Figure 2. a) Absorption spectra of pristine thin films of SiPCPDTBT, PFD1, and PCBM, and a thin film of the blend of SiPCPDTBT:PFD1. b) UPS spectrum of the secondary edge region. Inset is the HOMO region of PFD1.

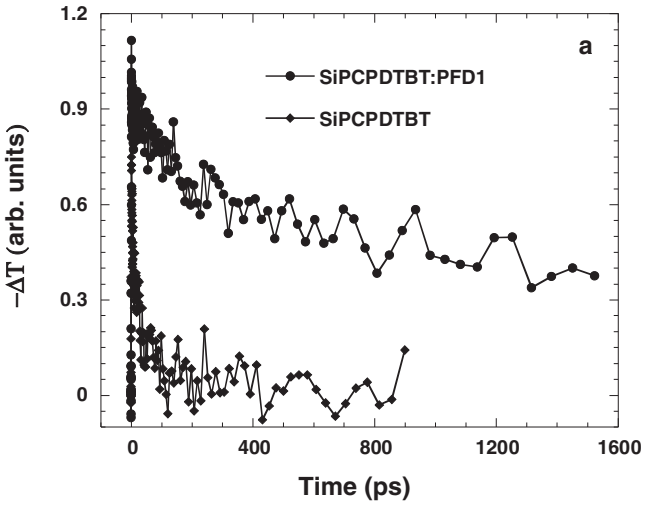

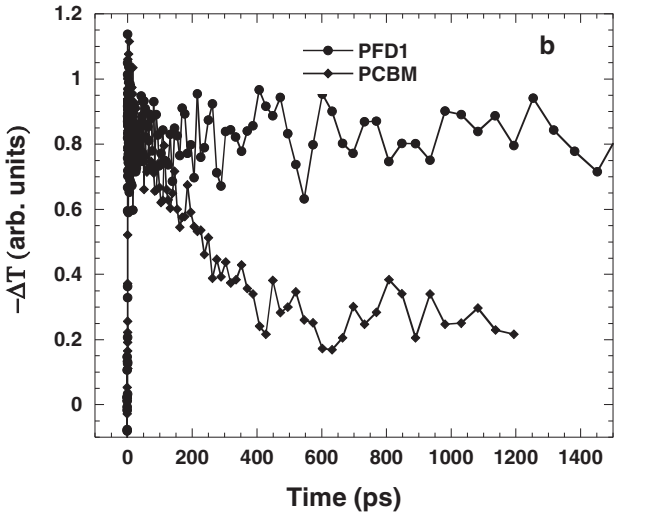

Figure 3. a) Mid-IR transient decay dynamics of SiPCPDTBT and SiPCPDTBT:PFD1 probed at 4.6 μm and pumped at 800 nm. b) The decay dynamics of PFD1 and PCBM pumped at 400 nm and probed at 480 nm.

have strong absorptions. Figure 3b compares the dynamics of the time-resolved PIA in pristine PFD1 and PCBM probed at 480 nm, where PCBM has strong absorption and PFD1 have negligible absorption. Compared to that in the PCBM, the much longer decay lifetime in PFD1 indicates the photogeneration of long-lived carriers, which is again consistent with efficient intermolecular charge transfer from porphyrin to fullerenes.[31–33] From these results, a high J_{sc} can be expected in PSCs made using porphyrin–fullerene dyads as the electron acceptor.

BHJ PSCs were fabricated with SiPCPDTBT:PFD1 in a device configuration of ITO/PEDOT:PSS/SiPCPDTBT:PFD1/Al, where ITO is indium tin oxide, PEDOT:PSS is poly(3,4-ethylene-dioxythiophene) (PEDOT), and PSS is poly(styrenesulfonate). The charge separating layer was a SiPCPDTBT:PFD1 blend with a 1:0.7 weight ratio. The thickness of active layer was ≈80 nm. The current–voltage (*J*–*V*) curve of the BHJ PSCs is shown in **Figure 4**. Under AM 1.5 G irradiation with 100 mW cm^{-2} intensity from a calibrated solar simulator, the SiPCPDTBT:PFD1 PSC yields J_{sc} of 13.6 mA cm^{-2} and V_{oc} of 0.66 V with a fill factor (FF) of 0.37 while the SiPCPDTBT:PCBM PSC yields J_{sc} of 11.5 mA cm^{-2} and V_{oc} of 0.56 V with a FF of 0.56. The PCE of the former in this case was determined to be 3.35%, which is slighty lower than the PSC made of SiPCPDTBT:PCBM (PCE = 4.03%) due to 34% lower value of the FF. Neverthelss, both its J_{sc} and V_{oc} are much higher, suggesting huge potential for future optimization to become an excellent electron acceptor. The high V_{oc} can be rationalized by the high LUMO of PFD1 measured by UPS (Figure 2b). More importantly, the large J_{sc}

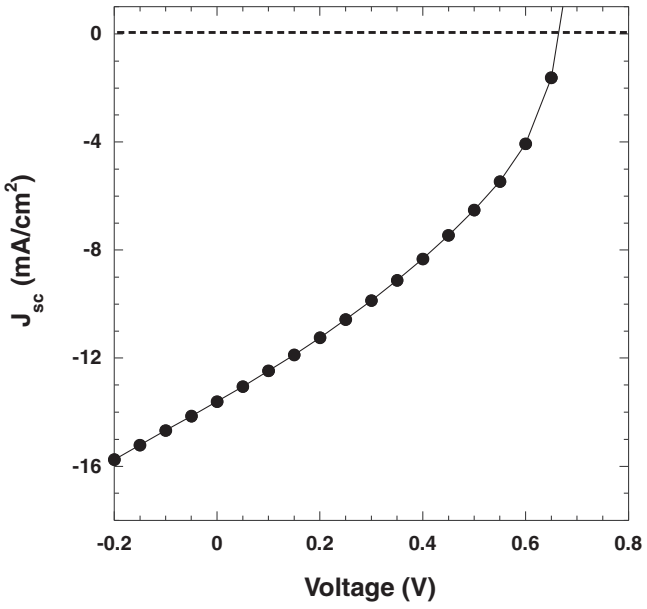

Figure 4. *J–V* characteristics of SiPCPDTBT:PFD1 PSCs under AM 1.5G illumination from a calibrated solar simulator with an intensity of 100 mW cm^{-2}.

implies that the straight and well-interacted C_{60} channels in the porphyrin–fullerene dyad with the supramolecular double-cable structure provides good hole and electron transporting properties in the PSCs. To prove that such a double cable structure still exists in the blend, thin-film samples of SiPCPDTBT:PFD1 blend (1.0:0.7) were prepared following a similar procedure for cell device fabrication and annealed at 135 °C for 16 h before transmission electron microscopy (TEM) observations. The ED pattern obtained in the blend film as shown in Figure S4a (Supporting Information) is identical to that of pure PFD1 in Figure 1b, indicating that the PFD1 ordered structure still remained in the thin-film blend. All the diffractions shown in Figure 1a,b and Figure S4a (Supporting Information) can be assigned to the (*hkl*) diffractions of the orthorhombic unit cell as listed in Table S1 (Supporting Information). Furthermore, the TEM bright field image illustrates the morphology of the columnar channels with a diameter around 10 nm embedded in the polymer matrix and locally oriented (Figure S4b, Supporting Information). This is an indicative of the intercolumnar C_{60} stacking of PFD1 in the blend. Taking into account of all the results, the PCEs of SiPCPDTBT:PFD1 PSCs can be substantially improved once the morphology is optimized.[3,5] Therefore, these results indicate the potential for improving PSCs performance via the manipulation of the supramolecular structure of π-conjugated molecules, in particular, the double cable structure.

In conclusion, a porphyrin–fullerene dyad, PFD1, was designed and synthesized to serve as a new electron acceptor. The structure, morphology, and electro-optical properties of PFD1 and its blend with SiPCPDTBT were studied and it was evaluated as a BHJ material. The dyad was found to self-organize into the supramolecular double-cable structure with the porphyrin forming the column via π–π interaction and the C_{60} moieties interacting intercolumnarly to form continuous C_{60} channels. Such a well-defined, alternating arrangement of continuous donor and acceptor domains is very promising as ambipolar transporting materials. PFD1 exhibits strong optical absorption over the spectral range from 300 nm to 600 nm. When blended with SiPCPDTBT, it improves the light harvesting in this spectral range. Ultrafast charge transfer and charge separation were observed both in pristine PFD1 and in the blends of SiPCPDTBT:PFD1. Photoinduced electron transfer from porphyrin to fullerene and from SiPCPDTBT to the porphyrin–fullerene dyad yields mobile carriers with long lifetimes. BHJ PSCs fabricated using SiPCPDTBT:PFD1 phase separated active layer exhibits higher J_{sc} and larger V_{oc}, as compared with that of PCBM, indicating that the double-cable structure is indeed an promising electron acceptor for high-performance PSCs.

Experimental Section

Materials Synthesis: The detailed descriptions are included in the Supporting Information.

Thermal Property Charaterization: The thermal analyses were characterized with a Perkin-Elmer PYRIS differential scanning caloremitry (DSC) with an Intracooler 2P apparatus. The temperature and heat flow scales were calibrated at a heating and cooling rate of 5 °C min^{-1} using standard materials. The thermogravimetric measurements were conducted on a TA TGA Q500 instrument at 10 °C min^{-1} in a nitrogen atmosphere.

Structural Charaterizations: For 2D WAXD patterns, a Rigaku 18 kW rotating anode X-ray generator attached to an R-AXIS-IV image plate system was used. The exposure time to obtain high-quality patterns was 45 min. The peak positions were calibrated using silver behenate in the low-angle region ($2\theta < 15°$), and silicon crystals in the high-angle region ($2\theta > 15°$). The crystal unit cells were determined by constructing reciprocal lattices. Computer refinement was conducted to find the solutions with the least error between the calculated values and the experimental results. TEM experiments were carried out with a Philips Tecnai 12 using an accelerating voltage of 120 kV. Selected area electron diffraction (SAED) patterns were obtained using a TEM tilting stage to determine the crystal structure parameters. The *d*-spacings were calibrated using a TlCl standard. Computer molecular modeling and analysis of the diffraction patterns were performed using the Cerius^2 package of Accelrys. Basic unit cell parameters determined by crystallographic experimental data from 2D WAXD and SAED experiments were used to build the crystallographic unit cell.

Ultraviolet Photoelectron Spectroscopy (UPS): For UPS measurements, a 100-nm-thick Au film was deposited on precleaned Si substrates with a thin native oxide. PFD1 solution in dichlororbenzene, 0.2% (w/v), was spin cast at spin speeds of 2000 rpm for 60 s. All films were fabricated inside a N_2 atmosphere glovebox and were transferred via an airtight sample holder to the UPS analysis chamber. Samples were also kept in a high vacuum chamber overnight to remove solvent residues. The UPS analysis chamber was equipped with a hemispherical electron energy analyzer (Kratos Ultra Spectrometer) and was maintained at 1×10^{-9} Torr. The UPS measurements were carried out using the He I ($h\nu = 21.2$ eV) source. During UPS measurements, a sample bias of –9 V was used in order to separate the sample and the secondary edge for the analyzer.

Time-Resolved Photoinduced Absorption: Films used for the time-resolved photoinduced absorption measurement were spin-cast onto sapphire substrates from a 2 wt% dichlororbenzene solution, either pure PFD1 or PCBM, resulting in a film thickness of ≈100 nm. The details of experimental setup and the measurements were previously reported.[31–33]

Bulk Heterojunction Polymer Solar Cells: Polymer solar cells were fabricated using SiPCPDTBT as the electron donor and PFD1 as the electron acceptor. The ITO-coated glass substrates were cleaned with

detergent, distilled water, acetone, and isopropyl alcohol in an ultrasonic bath and then dried overnight in an oven at >100 °C. After treatment of the ITO substrates with UV ozone for 40 min, highly conducting PEDOT:PSS was spin-cast from aqueous solution (5000 rpm, thickness of ≈40 nm). The substrates were dried at 160 °C for 10 min in air and transferred to a nitrogen-filled glovebox for spin-casting the SiPCPDTBT:PFD1 layer. Subsequently, a thin layer of the cathode, Al (150 nm), was thermally deposited on the BHJ layer through a shadow mask under vacuum. The area of the cathode that defined the active area of the device was 4.5 mm^2. All data were obtained under white light AM 1.5G illumination from a calibrated solar simulator with irradiation intensity of 100 mW cm^{-2}.

Supporting Information

Supporting Information is available from the Wiley Online Library or from the author.

Acknowledgements

This work was supported by the National Science Foundation (DMR-0906898) and the Collaborative Center for Polymer Photonics, AFOSR. The authors also thank Dr. Xiaopeng Li and Prof. Chrys Wesdemiotis for assistance with the MALDI-TOF mass spectra measurements.

Received: February 1, 2011
Revised: March 30, 2011
Published online: May 12, 2011

[1] C. J. Brabec, *Sol. Energy Mater. Sol. Cells* **2004**, *83*, 273.
[2] S. Günes, H. Neugebauer, N. S. Sariciftci, *Chem. Rev.* **2007**, *107*, 1324.
[3] C. J. Brabec, S. Gowrisanker, J. J. M. Halls, D. Laird, S. J. Jia, S. P. Williams, *Adv. Mater.* **2010**, *22*, 3839.
[4] W. Cai, X. Gong, Y. Cao, *Sol. Energy Mater. Sol. Cells* **2010**, *94*, 114.
[5] S. H. Park, A. Roy, S. Beaupre, S. Cho, N. Coates, J. S. Moon, D. Moses, M. Leclerc, K. Lee, A. J. Heeger, *Nat. Photonics* **2009**, *3*, 297.
[6] Y. Liang, Z. Xu, J. Xia, S. T. Tsai, Y. Wu, G. Li, C. Ray, L. Yu, *Adv. Mater.* **2010**, *22*, E135.
[7] M. C. Scharber, D. Muhlbacher, M. Koppe, P. Denk, C. Waldauf, A. J. Heeger, C. J. Brabec, *Adv. Mater.* **2006**, *18*, 789.
[8] G. Dennler, M. C. Scharber, T. Ameri, P. Denk, K. Forberich, C. Waldauf, C. J. Brabec, *Adv. Mater.* **2008**, *20*, 579.
[9] E. Wang, L. Wang, L. Lan, C. Luo, W. Zhuang, J. Peng, Y. Cao, *Appl. Phys. Lett.* **2008**, *92*, 033307.
[10] J. Hou, H. Y. Chen, S. Zhang, R. I. Chen, Y. Yang, Y. Wu, G. Li, *J. Am. Chem. Soc.* **2009**, *131*, 15586.
[11] Y. Liang, D. Feng, Y. Wu, S.-T. Tsai, G. Li, C. Ray, L. Yu, *J. Am. Chem. Soc.* **2009**, *131*, 7792.
[12] J. Peet, J. Y. Kim, N. E. Coates, W. L. Ma, D. Moses, A. J. Heeger, G. C. Bazan, *Nat. Mater.* **2007**, *6*, 497.
[13] R. B. Ross, C. M. Cardona, D. M. Guldi, S. G. Sankaranarayanan, M. O. Reese, N. Kopidakis, J. Peet, B. Walker, G. C. Bazan, E. Van Keuren, B. C. Holloway, M. Drees, *Nat. Mater.* **2009**, *8*, 208.
[14] J. E. Anthony, A. Facchetti, M. Heeney, S. R. Marder, X. Zhan, *Adv. Mater.* **2010**, *22*, 3876.
[15] F. G. Brunetti, X. Gong, M. Tong, A. J. Heeger, F. Wudl, *Angew. Chem.* **2010**, *49*, 532.
[16] A. Cravino, N. S. Sariciftci, *J. Mater. Chem.* **2002**, *12*, 1931.
[17] F. J. M. Hoeben, P. Jonkheijm, E. W. Meijer, A. P. H. J. Schenning, *Chem. Rev.* **2005**, *105*, 1491.
[18] R. Li, W. Hu, Y. Liu, D. Zhu, *Acc. Chem. Res.* **2010**, *43*, 529.
[19] H. Liu, J. Xu, Y. Li, Y. Li, *Acc. Chem. Res.* **2010**, *43*, 1496.
[20] L. C. Palmer, S. I. Stupp, *Acc. Chem. Res.* **2008**, *41*, 1674.
[21] T. Benincori, E. Brenna, F. Sannicoló, L. Trimarco, G. Zotti, P. Sozzani, *Angew. Chem.* **1996**, *108*, 718.
[22] J. P. Ferraris, A. Yassar, D. C. Loveday, M. Hmyene, *Opt. Mater.* **1998**, *9*, 34.
[23] A. Cravino, G. Zerza, M. Maggini, S. Bucella, M. Svensson, M. R. Andersson, H. Neugebauer, N. S. Sariciftci, *Chem. Commun.* **2000**, 2487.
[24] A. M. Ramos, M. T. Rispens, J. K. J. van Duren, J. C. Hummelen, R. A. J. Janssen, *J. Am. Chem. Soc.* **2001**, *123*, 6714.
[25] F. Zhang, M. Svensson, M. R. Andersson, M. Maggini, S. Bucella, E. Menna, O. Inganäs, *Adv. Mater.* **2001**, *13*, 1871.
[26] A. Cravino, G. Zerza, M. Maggini, S. Bucella, M. Svensson, M. R. Andersson, H. Neugebauer, C. J. Brabec, N. S. Sariciftci, *Monatsh. Chem.* **2003**, *134*, 519.
[27] M. Morana, H. Azimi, G. Dennler, H. J. Egelhaaf, M. Sharber, K. Forberich, J. Hauch, R. Gaudiana, D. Waller, Z. Z. Zhu, K. Hingerl, S. S. Bavel, J. Loos, C. J. Brabec, *Adv. Funct. Mater.* **2010**, *20*, 1180.
[28] R. J. P. Williams, *Chem. Rev.* **1956**, *56*, 299.
[29] W. R. Salaneck, M. Lögdlund, M. Fahlman, G. Greczynski, Th. Kugler, *Mater. Sci. Eng.* **2001**, *R34*, 121.
[30] J. H. Seo, T. Q. Nguyen, *J. Am. Chem. Soc.* **2008**, *130*, 10042.
[31] M. Tong, S. Cho, J. T. Rogers, K. Schmidt, B. B. Y. Hsu, D. Moses, R. C. Coffin, E. J. Kramer, G. C. Bazan, A. J. Heeger, *Adv. Funct. Mater.* **2010**, *20*, 3959.
[32] C. X. Sheng, M. Tong, S. Singh, Z. V. Vardeny, *Phys. Rev. B* **2007**, *75*, 085206.
[33] M. Tong, N. E. Coates, D. Moses, A. J. Heeger, S. Beaupre, M. Leclerc, *Phys. Rev. B* **2010**, *81*, 125210.